ELSEVIER

Journal of Alloys and Compounds 218 (1995) 31–35

Journal of ALLOYS AND COMPOUNDS

Investigation of the δ and μ phases in the Nd–Fe–Al system

J.M. Le Breton *, J. Teillet, D. Lemarchand, V. De Pauw

Laboratoire de Magnétisme et Applications, URA CNRS 808, Université de Rouen, F-76821 Mont-Saint-Aignan Cedex, France

Received 8 July 1994

Abstract

Nd–Fe–Al alloys containing either δ or μ phase (Al content in the 2.5–11 at.% range) were studied by X-ray diffraction analysis and Mössbauer spectrometry. A lattice expansion of the δ phase (composition $Nd_6Fe_{14-x}Al_x$) is observed, due to the substitution of Al for Fe in the $16l_2$ site of space group *I4/mcm*. The room-temperature Mössbauer spectrum is paramagnetic for $x=2.8$ and magnetic for $x=2$. For $x=2$, the mean iron moment is estimated to be 2.0 ± 0.1 μ_B. Room-temperature Mössbauer spectra of the μ phase ($Nd_{33.3}Fe_{66.7-x}Al_x$ with $x=5.3$ and 3.7) are magnetic, and the results support a slight distribution of environments around the Fe atoms due to the substitution of Al for Fe.

Keywords: Mössbauer spectrometry; Al substitution; X-ray diffraction

1. Introduction

In Nd–Fe–B-type sintered permanent magnets, the addition of aluminium improves the coercivity by modifying the microstructure. Aluminium increases the wettability of the Nd-rich intergranular phase during sintering, leading to a better magnetic deconnection of the grains of the hard magnetic $Nd_2Fe_{14}B$ phase [1]. On the other hand, new Nd–Fe–Al phases are formed in the grain boundaries, their influence on coercivity not being clearly established. A systematic study of the ternary Nd–Fe–Al diagram showed the presence of two stable phases below 600 °C, the so-called δ and μ phases, with the following compositions [2]:

δ phase: $Nd_{30}Fe_{70-x}Al_x$ with $8<x<25$,
μ phase: $Nd_{33.3}Fe_{66.7-x}Al_x$ with $2.5<x<5$.

These phases were observed in Al and in Al_2O_3-doped sintered Nd–Fe–B permanent magnets [3]. Recently, the presence of the μ phase was evidenced in an industrial Nd–Dy–Fe–Al–Co–B–V magnet [4].

In this paper, some results concerning the investigation of several samples containing either the δ phase or the μ phase are presented. We focused on the effect of the substitution of aluminium for iron.

2. Experimental

Five Nd–Fe–Al alloys, with different Al contents (in the range 2.5–11 at.%), were prepared at the Max Planck Institut (MPI), Stuttgart, Germany, and in our laboratory. The nominal compositions of the samples from the MPI were $Nd_{30}Fe_{60}Al_{10}$, $Nd_{37}Fe_{58}Al_5$, $Nd_{38}Fe_{58.5}Al_{3.5}$ and $Nd_{37}Fe_{60.5}Al_{2.5}$. They were prepared from Fe (99.99%), Nd (99.9%) and an Fe–Al prealloy of 50 at.% Fe and 50 at.% Al in an arc furnace and remelted several times for homogenization. The prealloy was melted from the pure elements Fe (99.99%) and Al (99.99%) by induction melting. The alloys containing the δ and μ phases were annealed at 580 °C for 60 and 30 days, respectively. In addition, we prepared an alloy with nominal composition $Nd_{33}Fe_{56}Al_{11}$ in an induction furnace. The starting material was Fe (99.98%), an Fe–Nd eutectic with 25 at.% Fe and 75 at.% Nd and Al (99.99%). The alloy was annealed for 30 days at 500 °C. The five alloys are listed in Table 1, with their designations.

Table 1
The different alloys and their designations

Alloy	Major phase	Designation
$Nd_{33}Fe_{56}Al_{11}$	δ	D1
$Nd_{30}Fe_{60}Al_{10}$	δ	D2
$Nd_{37}Fe_{58}Al_5$	μ	M1
$Nd_{38}Fe_{58.5}Al_{3.5}$	μ	M2
$Nd_{37}Fe_{60.5}Al_{2.5}$	μ	M3

---

* Corresponding author.

SSDI 0925-8388(94)01349-7

The samples were powdered and sieved (diameter less than 20 μm) for X-ray diffraction (XRD) and Mössbauer spectrometry analyses. XRD analysis was performed using a fast curved detector in an evacuated tank. The X-ray generator was equipped with a cobalt anticathode, using Co Kα radiation. The powders were analysed by reflection. Transmission ^{57}Fe Mössbauer spectrometry (TMS) analysis was performed between 4 K and room temperature using a conventional spectrometer with a source of ^{57}Co in a rhodium matrix. The samples contained about 10 mg cm^{-2} of natural iron. The compositions of the samples were measured by electron probe microanalysis (EPMA) at the MPI and at the School of Metallurgy and Materials, University of Birmingham, UK.

3. Results and discussion

3.1. Structural investigation of the δ phase

The XRD patterns of alloys D1 and D2 are shown in Fig. 1. The δ phase, observed in both alloys, is the only constituent of D2 (Fig. 1(a)). In D1, $Nd_2(Fe,Al)_{17}$ and $Nd(OH)_3$ are observed in addition to the δ phase (Fig. 1(b)). The hydroxide $Nd(OH)_3$ probably results from the oxidation in ambient air of the Nd phase observed previously in the same sample [5]. The peaks of the δ phase were indexed in the $Nd_6Fe_{13}Si$-type structure [6]. The lattice parameters of the δ phase, deduced from the measurement of the *d*-spacings, are reported in Table 2 and compared with the lattice parameters of the $Nd_6Fe_{13}Si$ and $Nd_6Fe_{11}Al_3$ compounds.

The measured compositions of the δ phase (see Table 2) show a higher Al content in D1. The lattice expansion of the δ phase in D1 is thus attributed to the substitution of Fe by Al, in agreement with the fact that the atomic radius of Al (0.143 nm) is higher than the atomic radius of Fe (0.126 nm). The highest lattice parameters are observed for $Nd_6Fe_{11}Al_3$ [7].

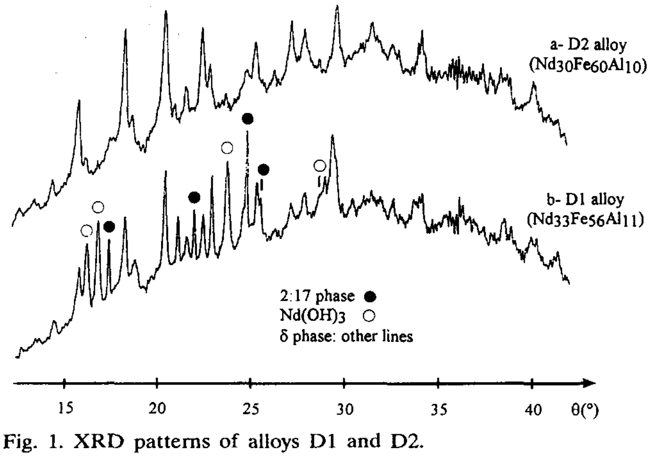

Fig. 1. XRD patterns of alloys D1 and D2.

Table 2
Lattice parameters of some $Nd_6Fe_{14-x}Al_x$ alloys, with those of $Nd_6Fe_{13}Si$ for comparison

Composition of δ phase	*a* (nm)	*c* (nm)	Ref.
$Nd_6Fe_{11}Al_3$	0.81472	2.30745	7
$Nd_6Fe_{11.2}Al_{2.8}$ (D1 alloy)	0.8098 ± 0.0010	2.299 ± 0.007	This study
$Nd_6Fe_{12}Al_2$ (D2 alloy)	0.8052 ± 0.0003	2.294 ± 0.003	This study
$Nd_6Fe_{13}Si$	0.8034	2.278	6

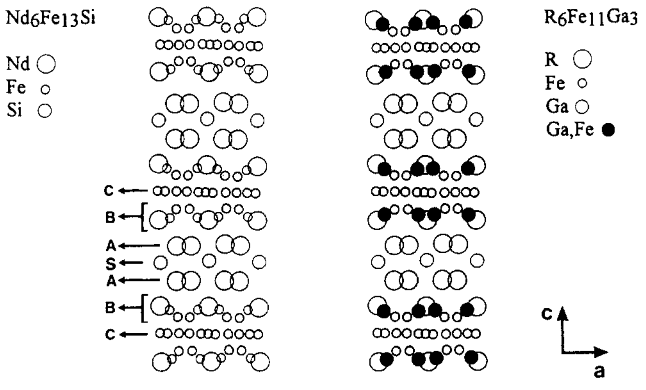

Fig. 2. Comparison of crystallographic structures of $Nd_6Fe_{13}Si$ and $R_6Fe_{11}Ga_3$ (after Refs. [6] and [8]).

Table 3
Number and mean distances (deduced from Ref. [6]) of the Nd and Fe nearest neighbours (NN) for each iron site in the $Nd_6Fe_{13}Si$ structure

Fe site	Fe NN	Nd NN
4*d*	12 (0.2472 nm)	0
16*k*	10 (0.2534 nm)	2 (0.3066 nm)
16*l*$_1$	9 (0.2546 nm)	3 (0.3095 nm)
16*l*$_2$	7 (0.2575 nm)	5 (0.3210 nm)

The $Nd_6Fe_{13}Si$ compound is an ordered version of $R_6Fe_{11}Ga_3$ (R = Pr,Nd,Sm) [8]. Its structure consists of a stacking of planes of Nd atoms (A type), Nd and Fe atoms (B type) and Fe atoms (C type) [6]. The sequence of planes along the *c* axis is CBASAB, where S is associated with a plane of Si atoms (see Fig. 2). The iron atoms occupy four different crystallographic sites. It must be noted that no Fe atom has an Si atom as a nearest neighbour. In Table 3 the number and mean distances (deduced from Ref. [6]) of the Nd and Fe nearest neighbours are reported for each iron site.

The $Nd_6Fe_{13}Si$ compound belongs to the tetragonal *I4/mcm* space group, while the $R_6Fe_{11}Ga_3$ compounds

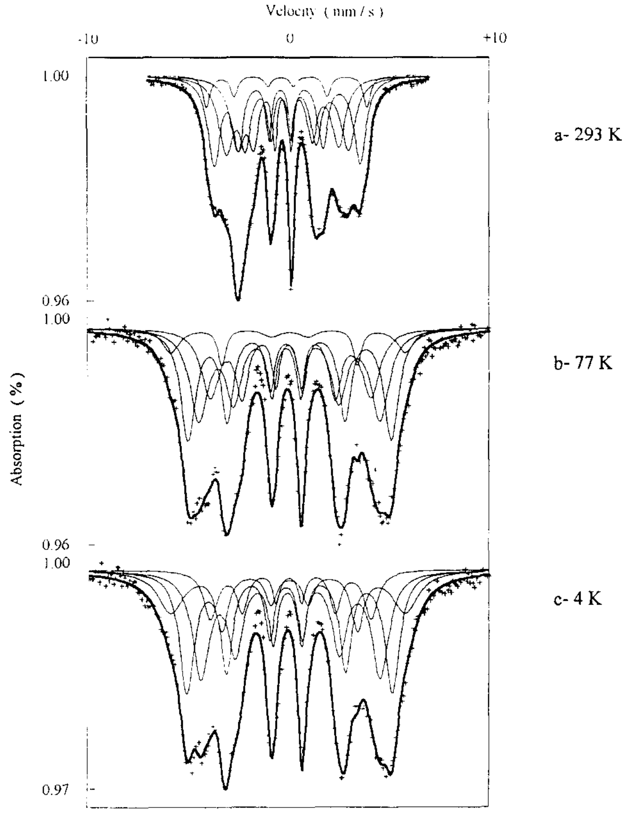

Fig. 3. Mössbauer spectra of alloy D2 ($Nd_{30}Fe_{60}Al_{10}$) at 293, 77 and 4 K.

belong to the tetragonal I42m space group. Assuming that the $16l_2$ iron site is occupied by both Fe and Ga, the *I4/mcm* space group can be deduced from the *I42m* space group [6]. This is illustrated in Fig. 2.

The amount of Al in the δ phase measured in sample D2 corresponds to the $Nd_6Fe_{12}Al_2$ composition. By considering that the site occupied by Si atoms in the $Nd_6Fe_{13}Si$ compound is filled with Al atoms, it must be considered that one Al atom is substituted for one Fe atom in $Nd_6Fe_{12}Al_2$. Taking into account that the atomic radius of Al is larger than that of Fe, we can suppose, as in the $Y_2Fe_{14}B$ phase [9], that the Al atom tends to occupy the site associated with the largest Fe–Fe mean distance, that is, the $16l_2$ iron site of space group *I4/mcm*. This assumption agrees with the fact that the $Nd_6Fe_{13}Si/R_6Fe_{11}Ga_3$ structural change is due to a modification of the occupancy of Fe and Ga (or Al) atoms on this site [7]. Thus the fact that Al substitutes easily for Fe in the $16l_2$ site can make difficult the formation of the $Nd_6Fe_{13}Al$ compound, for which there is no Al in the $16l_2$ site. The corresponding $Nd_{30}Fe_{65}Al_5$ phase does not belong to the homogeneous region [2]. The amount of Al associated with the upper limit of the homogeneous region would correspond to the $Nd_6Fe_9Al_5$ compound in which the $16l_2$ site would be filled with Al atoms.

3.2. Mössbauer investigation of the δ phase

The Mössbauer spectra of alloy D2 ($Nd_{30}Fe_{60}Al_{10}$, pure δ phase) at 293, 77 and 4 K are all magnetic (Fig. 3). They were fitted by four subspectra corresponding to the four crystallographic iron sites. In order to take into account the distribution of environments around each iron site due to the substitution of Al for Fe, the linewidths Γ of each subspectrum were fitted with the following constraints: $\Gamma_1=\Gamma_6\neq\Gamma_2=\Gamma_5\neq\Gamma_3=\Gamma_4$. No paramagnetic component was included. The components of each spectra were assigned to the iron sites by considering the nearest-neighbour environments. Assuming that the hyperfine field H_f is proportional to the number of iron neighbours, the following order is deduced: $H_f(4d)>H_f(16k)>H_f(16l_1)>H_f(16l_2)$. The fitted hyperfine parameters are listed in Table 4. The Mössbauer relative intensities *Int* agree well with the assumption that one Al atom is substituted for an Fe atom in the $16l_2$ site, which would lead to the theoretical values $Int(4d)=8.3\%$, $Int(16k)=Int(16l_1)=33.3\%$, $Int(16l_2)=25.0\%$. Assuming that the proportionality constant between the iron magnetic moment and the mean hyperfine field is 15 T μ_B^{-1}, the mean iron moment in $Nd_6Fe_{12}Al_2$ is estimated to be 2.0–2.1 μ_B.

The Mössbauer spectrum of alloy D1 ($Nd_{33}Fe_{56}Al_{11}$, containing both δ and 2:17 phases) at 293 K shows a magnetic contribution with broad lines and a paramagnetic peak at the centre (Fig. 4). According to the results of XRD, the spectrum results from the contributions of both δ and 2:17 phases. The measured composition of the 2:17 phase being $Nd_2Fe_{15}Al_2$, its Mössbauer contribution is magnetic at room temperature, with hyperfine fields higher than Nd_2Fe_{17} [10]. Thus the paramagnetic peak is attributed to the δ phase,

Table 4
Hyperfine field H_f (±0.5 T) and Mössbauer relative intensity *Int* (±2%) for each iron site of $Nd_6Fe_{12}Al_2$ compound (alloy D2) at 293, 77 and 4 K

Temperature (K)	*4d*		*16k*		$16l_1$		$16l_2$	
	H_f (T)	*Int* (%)	H_f (T)	*Int* (%)	H_f (T)	*Int* (%)	H_f (T)	*Int* (%)
293	24.9	7	22.7	32	19.0	32	15.7	29
77	36.8	9	32.0	33	28.5	33	25.3	25
4	38.8	10	33.9	33	29.6	32	26.7	25

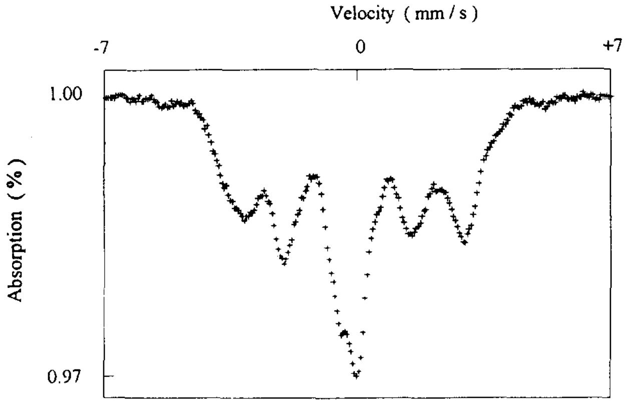

Fig. 4. Room-temperature Mössbauer spectrum of alloy D1 ($Nd_{33}Fe_{56}Al_{11}$).

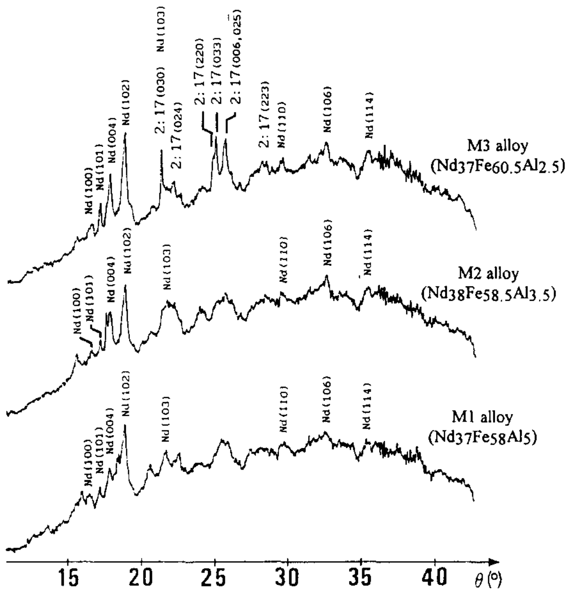

Fig. 5. XRD patterns of alloys M1, M2 and M3.

in accordance with its higher Al content (14 at.%) than in D2 (10 at.%).

This study shows that the room-temperature Mössbauer spectrum of the δ phase is not paramagnetic in all the homogeneity range. The room-temperature Mössbauer spectrum of the δ phase is magnetic for an Al content of 10 at.% (corresponding composition $Nd_6Fe_{12}Al_2$) and paramagnetic for Al contents of 14 at.% ($Nd_6Fe_{11.2}Al_{2.8}$), 15 at.% ($Nd_6Fe_{11}Al_3$) [7] and 20 at.% ($Nd_6Fe_{10}Al_4$) [11].

3.3. Mössbauer investigation of the μ phase

The structure of the μ phase has been studied in the alloy M2 [12]. It consists of a long-period stacking of planes, typical of polytypism. The XRD patterns of alloys M1, M2 and M3 are shown in Fig. 5. Sharp lines corresponding to metallic Nd are observed in all patterns. Sharp lines corresponding to the 2:17 phase are identified in the M3 diffraction pattern. Owing to its structure, the μ phase exhibits a very complex XRD pattern. The broad lines which are not indexed are thus attributed to the μ phase. The compositions of the phases are reported in Table 5.

The room-temperature Mössbauer spectra of M1 and M2, which correspond to pure μ phase, are very similar (see Fig. 6(a) and (b)). The room-temperature Mössbauer spectrum of M3 results from the contribution of both μ and 2:17 phases (see Fig. 6(c)). As the structure of the μ phase is still unknown, it is not possible to determine a definite fit to the Mössbauer spectrum. However, we found that a minimum set of

Table 5
Measured compositions of the intermetallic phases in alloys M1, M2 and M3

Alloy	Phase	Measured atomic composition
$Nd_{37}Fe_{58}Al_5$ (M1)	μ	$Nd_{33.3}Fe_{61.4}Al_{5.3}$
$Nd_{38}Fe_{58.5}Al_{3.5}$ (M2)	μ	$Nd_{33.3}Fe_{63.0}Al_{3.7}$
$Nd_{37}Fe_{60.5}Al_{2.5}$ (M3)	μ	$Nd_{33.3}Fe_{63.3}Al_{3.4}$
	2:17	$Nd_2Fe_{16.7}Al_{0.3}$

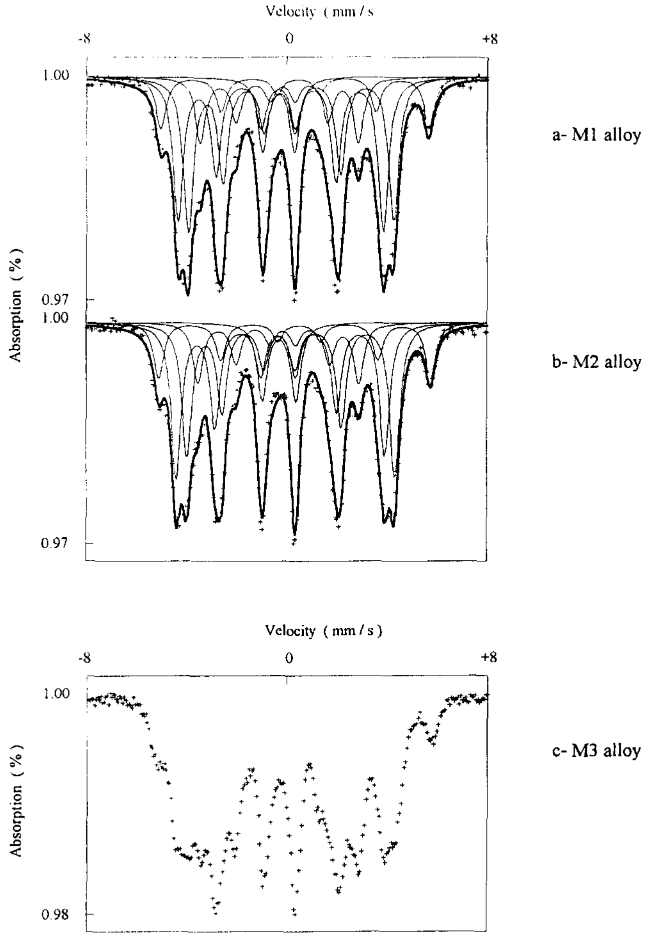

Fig. 6. Room-temperature Mössbauer spectra of alloys M1 ($Nd_{37}Fe_{58}Al_5$), M2 ($Nd_{38}Fe_{58.5}Al_{3.5}$) and M3 ($Nd_{37}Fe_{60.5}Al_{2.5}$).

Table 6
Room-temperature hyperfine parameters (hyperfine field H_f, isomer shift *IS*, quadrupolar shift 2ϵ, quadrupolar splitting *QS*) and Mössbauer relative intensity *Int* of alloys M1 ($Nd_{37}Fe_{58}Al_5$) and M2 ($Nd_{38}Fe_{58.5}Al_{3.5}$) [a]

Subspectrum	H_f (T)		*IS* (mm s^{-1})		2ϵ, QS (mm s^{-1})		*Int* (%)	
	M1	M2	M1	M2	M1	M2	M1	M2
1	33.3	33.7	0.48	0.51	−0.14	−0.20	11.4	12.7
2	26.8	27.1	−0.09	−0.10	0.30	0.30	32.0	35.0
3	24.3	24.6	−0.07	−0.07	0.25	0.26	34.5	30.0
4	19.7	20.0	−0.15	−0.15	−0.11	−0.18	13.8	13.5
Paramagnetic	–	–	−0.23	−0.21	1.28	1.34	8.3	8.8

[a] Values of *IS* are relative to α-Fe. Fitted linewidths Γ are 0.52 and 0.48 mm s^{-1} for M1 and M2, respectively. Errors for hyperfine parameters are ±0.5 T for H_f and ±0.02 mm s^{-1} for *IS*, 2ϵ and *QS*.

four magnetic subspectra is required to obtain a good fit. The spectra of M1 and M2 were fitted in a simple way by four magnetic subspectra with equal linewidth. A paramagnetic component was included in order to take into account the excess absorption in the two central lines of both spectra. Its physical signification is rather doubtful. The fitted hyperfine parameters are listed in Table 6. The mean hyperfine field is lower for M1 (23.5 T) than for M2 (23.8 T), in agreement with the higher Al content in M1. The large values of the fitted linewidths agree with a slight distribution of environments around the iron atoms. The linewidth is higher for M1 than for M2, supporting a higher distribution of environments around the iron sites in the compound containing the highest Al content. The complete analysis of the Mössbauer spectrum requires a better knowledge of the crystallographic structure of the μ phase.

4. Conclusions

Structural and Mössbauer analyses of the δ phase of the system Nd–Fe–Al (composition $Nd_6Fe_{14-x}Al_x$) showed that Al substitutes for Fe in the $16l_2$ site of space group *I*4/*mcm*. The room-temperature Mössbauer spectrum is paramagnetic for $x = 2.8$, in agreement with the results obtained for $x = 3$ [7], and magnetic for $x = 2$, with a mean hyperfine field of 19.6 T. The mean iron moment in $Nd_6Fe_{12}Al_2$ is estimated to be 2.0–2.1 μ_B.

Room-temperature Mössbauer analysis of the μ phase (composition $Nd_{33.3}Fe_{66.7-x}Al_x$) was performed for $x = 5.3$ and $x = 3.7$. Both spectra are magnetic with mean hyperfine fields of 23.5 and 23.8 T, respectively. The results support a slight distribution of environments around the Fe atoms, due to Al substitution for Fe.

Acknowledgements

This work forms part of the Concerted European Action on Magnets (CEAM), supported by the BRITE/EURAM program of the European Commission. The authors acknowledge B. Grieb for providing the samples prepared at the MPI and D. Edgley (School of Metallurgy and Materials, University of Birmingham) for the EPMA measurements of the δ phase.

References

[1] K.G. Knoch, G. Schneider, J. Fidler, E.Th. Henig and H. Kronmüller, *IEEE Trans. Magn.*, *25* (1989) 3426.
[2] B. Grieb, *Thesis*, Stuttgart, 1991.
[3] K.G. Knoch, B. Grieb, E.Th. Henig, H. Kronmüller and G. Petzow, *IEEE Trans. Magn.*, *26* (1990) 1951.
[4] L. Legras, J. Delamare, D. Lemarchand, J. Vu-Dinh and P. Vigier, *J. Alloys Comp.*, accepted for publication.
[5] V. De Pauw, unpublished results.
[6] J. Allemand, A. Letant, J.M. Moreau, J.P. Nozières and R. Perrier de la Bâthie, *J. Less-Common Met.*, *166* (1990) 73.
[7] B.P. Hu, J.M.D. Coey, H. Klesnar and P. Rogl, *J. Magn. Magn. Mater.*, *117* (1992) 225.
[8] O.M. Sichevich, R.V. Lapunova, A.N. Sobolev, Y.N. Grin' and Y.R. Yarmolyuk, *Kristallografiya*, *30* (1985) 1077.
[9] Y.C. Yang, D. Tharp, G.J. Long, O.A. Pringle and W. James, *J. Appl. Phys.*, *61* (1987) 4343.
[10] W.B. Yelon, H. Xie, G.J. Long, O.A. Pringle, F. Grandjean and K.H.J. Buschow, *J. Appl. Phys.*, *73* (1993) 6029.
[11] R. Politano, A.C. Neiva, H.R. Rechenberg and F.P. Missel, *J. Alloys Comp.*, *184* (1992) 121.
[12] J. Delamare, D. Lemarchand and P. Vigier, *J. Magn. Magn. Mater.*, *104–107* (1992) 1092.